Theory and Practice of Science and Technology
2025, VOL. 6, NO. 2, 21-27
DOI: 10.47297/taposatWSP2633-456905.20250602

A refined modeling and analysis method for single and multi rotor targets

Yuanduo Niu

Xi'an Electronic Engineering Research Institute, Xi'an, 710000, China

ABSTRACT
For helicopter targets, rotor blades are usually simplified as multiple scattering points on a straight line, but in reality, rotor blades have a width and there may be differences in RCS when approaching and moving away from the blades. Therefore, it is necessary to explore more refined modeling methods for rotor blades to approach real targets more closely. This article proposes a more refined modeling method to simulate the time-frequency changes of helicopter rotor blades approaching and moving away from radar in real life, which can improve the feature extraction ability of helicopter and unmanned aerial vehicle targets. Comparison of measured data is conducted to improve the application performance of radar systems in the field of communication.

KEYWORDS
Rotary wing unmanned aerial vehicle; Modeling; radar; micro-Doppler

1 Introduction

Micro-motion refers to the movements of a target excluding the motion of the main body, including rotation, vibration, rolling, and precession. The relative motion of the target with respect to the radar induces modulation effects on the radar echoes, specifically the Doppler effect. This effect results in a significant change in the frequency of the radar echoes compared to the transmitted wave, with the frequency variation defined as the Doppler frequency. After scattering the radar wave from the target's main body, the carrier frequency center experiences a Doppler shift[1]. Subsequently, when the radar wave is scattered by micro-motion components that undergo periodic rotation or vibration, sideband Doppler shifts occur, leading to the generation of micro-Doppler effects. The frequency-modulated signal resulting from these sideband Doppler shifts is referred to as the micro-Doppler (m-D) signal[2]. Significant progress has been made both domestically and internationally in modeling radar micro-motion targets. Based on the point scatterer model assumption, V. C. Chen conducted mathematical modeling, theoretical derivation, and simulation studies on four typical forms of micro-motion—rotation, vibration, rolling, and coning—and their resultant micro-Doppler effects[3]. Thayaparan[4] performed field tests with corner reflectors, obtaining results consistent with theoretical predictions. For simple forms of micro-motion such as rotation, vibration, and rolling, the motion along the radar line-of-sight (LOS) can be described as simple harmonic motion[5]. For instance, the time-frequency analysis results of radar echoes collected from a single scatter point target (metal sphere) undergoing rotational motion in a darkroom environment. It is evident that the micro-Doppler frequency of the target is related to its micro-motion frequency, micro-motion amplitude, and LOS, exhibiting a sinusoidal frequency modulation (SFM) signal pattern over time, which also reflects a sinusoidal variation in the time-frequency image.

In practice, micro-motion targets often do not conform to the isotropic ideal point scatterer model assumption. Variations in the scattering center's position and intensity during micro-motion can nonlinearly modulate the echo amplitude. Therefore, it is essential to consider factors such as target attitude changes, target shape, echo discontinuities, and occlusion effects in real-world applications. Additionally, the parameters of the radar transmitted signal can influence the observation of micro-Doppler frequencies[6]. Literature has proposed a dynamic simulation method to study the electromagnetic scattering of tilt-rotor aircraft during multi-mode continuous flight. This method establishes a time-varying mesh approach to represent the dynamic rotation of the rotorcraft. It calculates the radar cross-section (RCS) using emitted and reflected rays alongside uniform diffraction theory. By extracting micro-Doppler and inverse synthetic aperture radar (ISAR) images, the scattering mechanism of rotorcraft has been investigated. However, these methods do not address the RCS fluctuations that occur when helicopter rotor blades approach and recede from the radar, which can significantly affect subsequent echo separation, feature extraction, and imaging results.

2 Materials and methods

A Helicopter single rotor dual line echo model

As shown in Figure 1, when extending the model to the helicopter target, the helicopter flies along a straight trajectory parallel to the OX axis at a constant height, with a constant velocity V_t. The rotor blades rotate on a horizontal plane parallel to the XOY plane. Let the coordinates of the rotor center at the initial moment be defined as C_V:(x_0,y_0,z_0). The rotor's rotational speed is denoted as f_r, and $R_0$is the distance from the radar center to the rotor's rotational center. Each rotor blade comprises N blades, with a spacing of $\Delta\phi = 2\pi/N_L$ between adjacent blades.

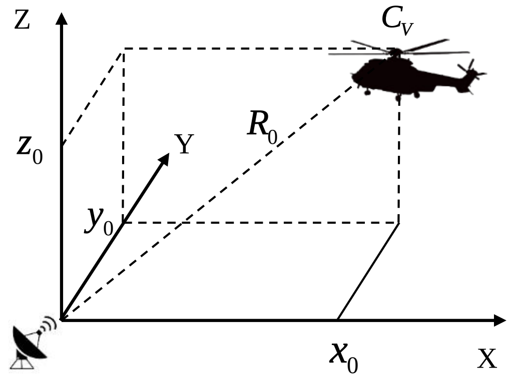

Figure 1 Helicopter Movement Diagram

For helicopters, typical helicopter blades have a certain blade width, as shown in the measured data Robinson R44 used in this article, whose blade model is shown in Figure 2:

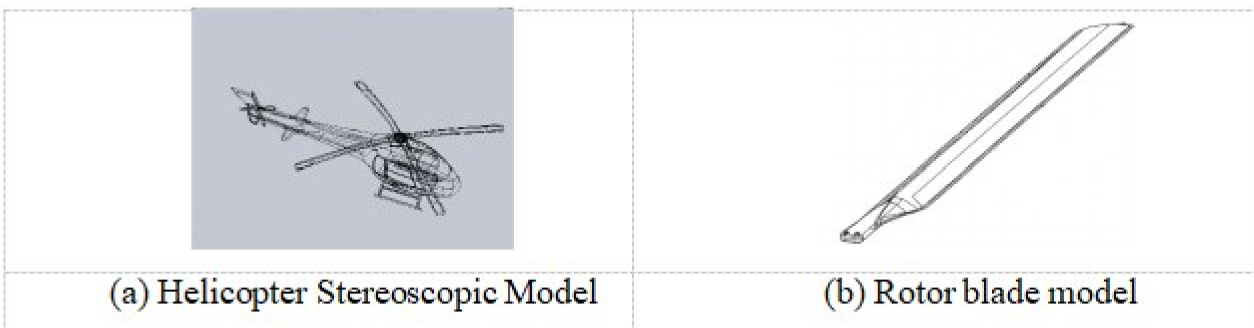

Figure 2 Helicopter and rotor blade models

As shown in Figure 2, the helicopter rotor blades possess a certain width. Taking the Robinson R44 as an example, the blade width is 20 cm. According to the equivalent model of radar target characteristics, the helicopter blade can be modeled as a metallic flat plate, where the scattering points are distributed along two straight lines that correspond to the edges of the rotor blades. The spacing between these scattering points is denoted as λ/4.

In this paper, this model will be referred to as the dual-line model of helicopter blades. Additionally, there is a section of the rotor hub that connects the rotor blades to the rotor center, which does not contain any rotor blades. Therefore, when constructing the model, the scattering point locations should commence from a position onward, where $R_{\min}$ represents the length of the non-blade section.

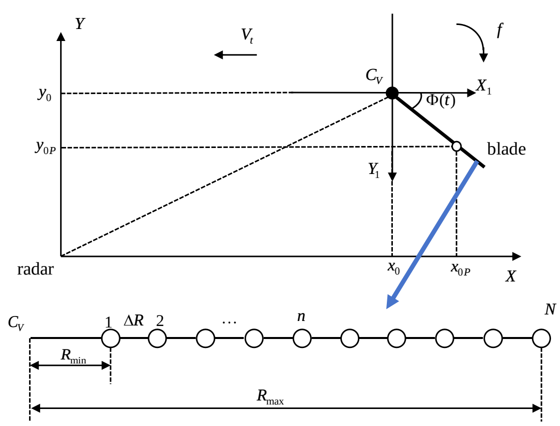

Figure 3 Double line model construction

As shown in Figure 3, the rotor blades are equivalent to a metal plate, and their scattering points can be set as two straight lines at the leading and trailing edges of the blades. If so, the coordinates of the scattering point can be expressed as:

$$x'_{L,R}(t) = x_0 + V_t t + R_n \cos(\phi_n(t)) + L_b \sin(\phi_n(t)) \tag{1}$$

$$y'_{L,R}(t)=\begin{cases} y_0 - R_n \sin(\phi_n(t)) + L_b \cos(\phi_n(t)), \text{clockwise} \\ y_0 + R_n \sin(\phi_n(t)) - L_b \cos(\phi_n(t)), \text{anticlockwise} \end{cases} \tag{2}$$

$$z'_{L,R}(t)=z_0 \tag{3}$$

Among them, $L_b$is the width of the helicopter blades. The distance between the scattering point and the radar can be expressed as:

$$r_{L,R}(t)=\sqrt{x'^2_{L,R}(t)+y'^2_{L,R}(t)+z'^2_{L,R}(t)} \tag{4}$$

If the blade position meets the requirements:

$$\frac{\pi}{2} \leqslant \phi_n(t) \leqslant \frac{3}{4}\pi \tag{5}$$

The blade moves away from the radar and reflects its trailing edge. If the blade position meets the requirements:

$$0 \leqslant \phi_n(t) < \frac{\pi}{2} \| \frac{3}{4}\pi < \phi_n(t) \leqslant 2\pi \tag{6}$$

Thus, the modulated echo complex vector synthesized by P scattering centers can be expressed as follows:

$$s(t)=\sum_{k=1}^{P} \sigma_k \exp(j\psi_k(t)) \tag{7}$$

Among them, σ_k is the amplitude function of the k-th scattering center scattering, and $\psi_k(t)$ is the phase function of the k-th scattering center scattering.

The blade approaches the radar and reflects its leading edge. The maximum Doppler frequency of a helicopter should be the maximum micro Doppler frequency of the blade tip, also known as the tip velocity:

$$f_{d\max}=\frac{2v_{\max}}{\lambda}\cos\beta=\frac{4\pi f_r R_L}{\lambda}\cos\beta \tag{8}$$

Due to the expression of the rotor echo, it can be seen that the modulation effect of blade rotation on the echo is manifested as a periodic "flicker" phenomenon in the time domain, and the shape of the "flicker" is a sinc function. The interval of the "flicker" period in the time domain depends on the rotor speed and the number of blades on the rotor:

$$T=\frac{1}{nf_r} \tag{9}$$

The modulation effects of rotor targets on radar echoes are manifested in the frequency domain as a series of equidistant spectral lines[7]. The spacing between these spectral lines (modulation period) is solely determined by the number of rotor blades and the rotor blade rotation frequency f_r.

Thus, the frequency domain modulation characteristics of helicopter rotor blades can be summarized by three key parameters: the spacing between spectral lines, the one-sided spectral width, and the number of one-sided spectral lines, which are defined as follows:

$$f_T=Nf_r \tag{10}$$

$$B_1=\frac{2v_{\max}}{\lambda}\cos\beta=\frac{4\pi f_r l}{\lambda}\cos\beta \tag{11}$$

$$N_1=\frac{B_1}{f_T}=\frac{4\pi l\cos\beta}{\lambda N} \tag{12}$$

In summary, the rotation of the rotor blades modulates the radar echoes, which manifests in the time domain as a “flicker” shaped like a sinc function that occurs at a period T. In the frequency domain, it appears as spectral lines centered around the Doppler frequency shift corresponding to the body’s radial motion, with a spacing defined by f_T and a one-sided spectral width of B_1. The following sections analyze the causes of this modulation phenomenon from both the time and frequency domains.

For the time-domain echoes, when the rotor blades are positioned perpendicularly to the radar line of sight during their rotation, the radar echo amplitude reaches its maximum. As the rotors continue to rotate, the position of the blades relative to the radar and the effective reflective area both change. This change occurs abruptly rather than continuously, resulting in a rapid decrease in echo amplitude.

Regarding the Doppler-domain echoes, the time-domain signal corresponds to a sampling process of the fixed position blades perpendicular to the radar line of sight at periodic intervals T. Consequently, impulses are generated at the corresponding Doppler frequency shifts associated with the body’s radial motion. These impulse signals periodically extend in the Doppler domain with intervals of 1/T towards both sides, causing the modulated echoes of the rotor to manifest as equidistant spectral lines in the frequency domain.

Furthermore, since the lengths of the rotor blades and their angular frequency are constant, all scattering points along the rotor blades will exhibit the same maximum radial velocity. As a result, the modulated echoes in the Doppler domain will not extend infinitely towards either side.

For unmanned aerial vehicles (UAVs), which typically have multiple rotors, this paper focuses on the modeling of multi-rotor UAVs.

Figure 4 Drone model

As shown in Figure 4, the XT9 aerial drone has four rotors, each with two blades, but the blade width is often less than 3cm, so its blades are equivalent to a straight line. The echo signal generated by a single rotor of the drone is

$$s_r(t)=\sum_{n_L=1}^{N_L}\sum_{n_R=1}^{N_R} s(t-t_d)\sigma_k \exp(j(2\pi f_0 t+\varphi(t))) \tag{13}$$

If there are multiple rotors, the echo signals of multiple rotors will be superimposed, and the only difference is that the initial angles of the blades of different rotors are different.

$$s(t)=\sum_{n=1}^{N_r} s_n(t) \tag{14}$$

Among them, N_r represents the number of rotors of the drone, and $s_n(t)$represents the radar echo signal generated by the n-th rotor.

Through these steps, precise modeling of helicopters and rotary wing drones can be achieved, effectively simulating the signals of the main body and rotating components in radar echoes.

I. Results & Discussion

Based on the relevant derivation and theoretical analysis of the modulated echo models for helicopters and drones mentioned above, simulation signals are used to verify the above conclusions. Firstly, verify the helicopter,

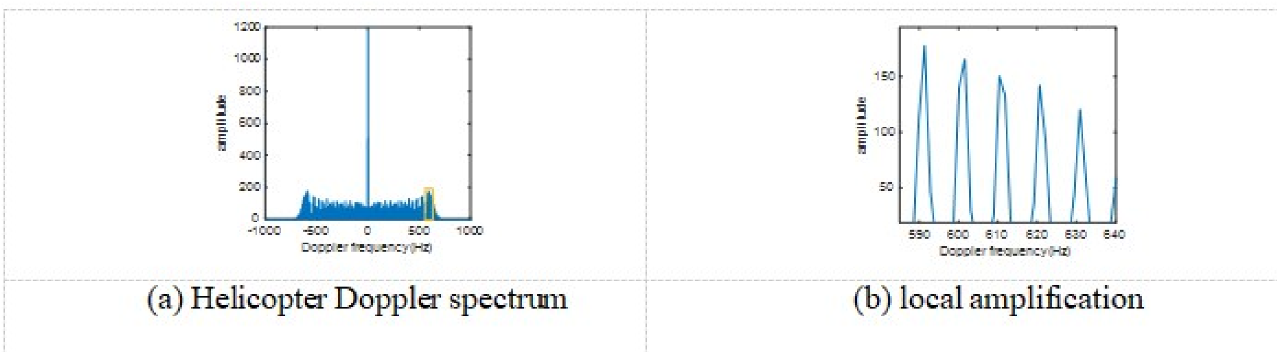

Figure 5 Simulate the Doppler spectrum of a single point model

As illustrated in Figure 5 the Doppler spectrum of the simulated single scatter point model shows a spectral line spacing of $f_r \cdot N_L$. The calculation formula for the one-sided Doppler spectrum is represented as $f_{d\max}=4\pi f_r R_L/\lambda$Hz. Through the number of spectral lines and the given simulation parameters, the spectral line spacing in the Doppler domain for the simulated signal is derived to be $f_T=10$Hz using Equation (10). Consequently, the modulation characteristics of the complex envelope in the time domain correspond to a pulsed signal with a modulation period of T seconds. This modulation exhibits a "flickering" peak in the time domain when the rotor blades are perpendicular to the radar line of sight, as shown in Figure 5. The modulation period T is determined to be 0.1208 s, aligning with the theoretical derivation in Equation (10) and the analysis above.

Utilizing Equations (11) and (12) with the simulation parameters, the theoretical values for the one-sided spectral line count and one-sided spectral width are obtained as $N_1=B_1$ respectively. These results are consistent with the one-sided spectral width and spectral line count presented in Figure 5, thereby validating the reasonableness of the theoretical derivation of the micro-Doppler effect in the Doppler domain.

Given that the helicopter blades should be modeled as an aggregation of multiple scattering points, we can compare images obtained from the refined modeling of the helicopter with those from the initial modeling approach. This comparison serves to illustrate the improved accuracy in representing the radar scattering characteristics of the helicopter blades when employing a more detailed modeling strategy.

(a) Helicopter rotor blade time-frequency diagram

(b) Helicopter rotor blade video diagram (refined)

Figure 6 Comparison of time-frequency diagrams before and after helicopter fine modeling

Similarly, in the time-frequency domain, it can be clearly observed that the micro Doppler of rotors with even and odd blades is different. The micro Doppler of even numbered blades is symmetrical with the main frequency, but the results of odd numbered blades are not symmetrical. However, if equivalent to a dual line model, it can be seen that the amplitude of the target rotor changes due to the variation of rotor RCS when approaching and moving away from the radar. As shown in Figure 6(b), the time-frequency diagram of the dual line model helicopter clearly shows the difference in amplitude when the blades approach and move away from the radar.

Next, simulation analysis will be conducted on the drone. The simulated drone consists of four rotors, each with two blades. The time-frequency and Doppler spectra are shown below:

(a) Time frequency diagram of rotary wing unmanned aerial vehicle

(b) Doppler spectrogram of rotary wing unmanned aerial vehicle

Figure 7 Time frequency and Doppler spectra of unmanned aerial vehicles

As shown in Figure 7,the spectral line spacing is observed to be 20 Hz, which corresponds to the expected value. The time-frequency representation exhibits four peaks, each corresponding to one of the four rotor blades. The simulation settings specify that each pair of blades has an initial rotational angle difference of 30 degrees. With a rotor speed of 10 r/s, the rotation period is 0.1 s, resulting in a time interval of 8.3 ms between adjacent blades, which aligns with the simulation results.

Now, we proceed to analyze the measured data collected from an S-band radar during outdoor field experiments, with the target being the Robinson R44 helicopter (USA, Thunderbird Raven II). The known radar parameters and target parameters are summarized in Table 1 below:

Table 1 Radar parameters and target parameters

Parameter	value	unit
carrier frequency	3.13344	GHz
bandwidth	120	MHz
Pulse width	2.08	μs
Pulse repetition frequency	3.72	kHz

Based on the above radar and target parameter settings, field experimental data collection was carried out. In order to meet the requirement of Doppler non aliasing, a hovering echo data segment with a fixed height of 50 m at 300 m was taken for analysis. The measured R44 Doppler domain modulation spectrum and time-frequency analysis results of the helicopter are shown in Figure 8:

(a) Doppler domain results of helicopter measured data

(b) local amplification

Figure 8 Doppler spectrum of Robinson R44

(a) Time frequency analysis of helicopter measured data

(b) local amplification

Figure 9 Time frequency diagram of Robinson R44

As shown in Figure 8, by substituting the actual parameters into Equations (11) and (12), the theoretical values for the one-sided spectral line count and the one-sided spectral width are obtained as $N_1 = 306$and $B_1 = 1582.9$Hz, respectively. These values are consistent with the observed one-sided spectral width and spectral line count presented in the Doppler domain.

From the analysis above, the maximum micro-Doppler frequency shift is calculated to be 1582.9 Hz, which is in close agreement with the measured value$f_{d\max} = 1457.1$Hz shown in Figure 8. As shown in Figure 9, it is noteworthy that, due to the target being in a hovering state, the modulation components generated by the rotor are distributed symmetrically around the strong main echo. The asymmetry observed in the positive and negative frequencies is attributed to the physical structure of the helicopter rotor. This structure results in variations in the scattering area as the target approaches or recedes from the radar.

Overall, the empirical data validate the theoretical reasoning regarding the micro-Doppler effect in the Doppler domain. The Doppler spectrum and time-frequency plot of the DJI longitude and latitude M300 are shown below:

(a) Doppler domain results of measured data of DJI longitude and latitude M300

(b) local amplification

Figure 10 Doppler spectrum of DJI longitude and latitude M300

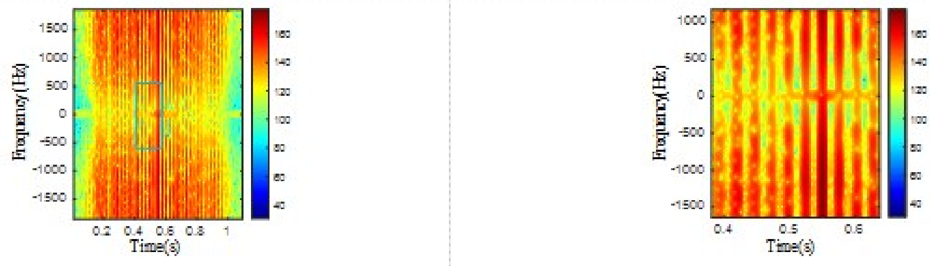

(a) Time frequency analysis of measured data of DJI longitude and latitude M300

(b) local amplification

Figure 11 Time frequency map of DJI longitude and latitude M300

As shown in Figure 10, the Doppler spectrum of the DJI Matrice 300 exhibits a spectral line spacing of approximately 90 Hz. This spacing is attributed to the fact that when the DJI Matrice 300 is in a hovering state, its rotor speed is$f_r = 45$r/s, and it has $N_L = 2$ blades. Therefore, the spectral line spacing can be derived as follows: $f_{d\max} = 4\pi f_r N_L/\lambda$.Moreover, based on the formula for calculating the maximum one-sided Doppler frequency, a value of 1903 Hz is computed, which corresponds to the data presented in the Figure 9.

In Figure 11, the time-frequency representation shows multiple peaks, each corresponding to signals generated by the different rotor blades. This indicates the presence of individual micro-Doppler signatures attributed to the unique rotational characteristics of each blade during the UAV's operation. This information is crucial for understanding the radar scattering behavior of the UAV and its implications in radar signal interpretation.

3 Conclusions

This paper analyzes the mechanical structural parameters and motion state information of helicopters and unmanned aerial vehicles (UAVs). Based on this analysis, a detailed mathematical modeling and theoretical derivation of radar echo signals under ideal conditions are conducted. The study investigates the modulation effects of micro-movement targets in the frequency domain, Doppler domain, and time-frequency domain under various radar parameters and target physical parameters. The modulation characteristics, such as spectral spacing and spectral broadening, are verified. Furthermore, the research delves into the impact of the dual-line model for helicopters and the UAV model on micro-Doppler characteristics. This work is significant for understanding the separation of micro-movement target echoes and imaging of rotating components.

References

[1] Han, Lixun; Feng, Cunqian. Parameter Estimation for Precession Cone-Shaped Targets Based on Range–Frequency–Time Radar Data Cube.[J]. Remote Sensing,2022,14(7): 1548.

[2] Haobo Wang; Yingxi Liu; Lei Ni; Ying Luo. Micro-Doppler effect removal in inverse synthetic aperture radar imaging based on UNet[J]. Electronics Letters, 2023,59(9): e12814.

[3] NgocBinh N, MinhNghia P, Van-Sang D. Improving Human Activity Classification Based on Micro-doppler Signatures of FMCW Radar with the Effect of Noise[J]. PloS one, 2024, 19(8): 1932-6203.

[4] Thayaparan T, Stanković L, Djurović I. MicroDoppler-based Target Detection and Feature Extraction in Indoor and Outdoor Environments[J]. Journal of the Franklin Institute, 2008, 345(6): 700-722.

[5] Chen V C, Li F, Ho S S, et al. Micro-Doppler Effect in Radar: Phenomenon, Model, and Simulation Study[J]. IEEE Transactions on Aerospace and Electronic Systems, 2006, 42(1):2-21.

[6] Zhongyang F, Yan Y, Xiangwen J. Dynamic Electromagnetic Scattering Simulation of Tilt-Rotor Aircraft in Multiple Modes[J]. Sensors, 2023, 23 (17): 76-78.

[7] Wu Q, Sherman D. Boundary Extension and Stop Criteria for Empirical Mode Decomposition[J]. Advances in Adaptive Data Analysis, 2010, 2(2): 157-169.